Theory of Raman scattering in superconductors

M. V. Klein and S. B. Dierker*
Department of Physics and Materials Research Laboratory, University of Illinois at Urbana—Champaign, 104 S. Goodwin Avenue, Urbana, Illinois 61801

(Received 8 August 1983; revised manuscript received 13 January 1984)

The electronic Raman scattering by pairs of quasiparticles is calculated at zero temperature, generalizing previous calculations that were based on the Bardeen-Cooper-Schrieffer model of a superconductor. Analytical and numerical results are presented for the spectrum as a function of wave vector $\vec{q}$, and an integration is performed over q_z to include the effect of a finite optical penetration depth. Allowing for gap anisotropy, we correct the results for vertex and Coulomb polarization effects. The theoretical results for finite q are used to calculate spectra for Nb_3Sn, V_3Si, and Nb, neglecting gap anisotropy. Experimental data are presented for V_3Si and Nb. The data for V_3Si are fit to a zero-q theory that includes gap anisotropy, with results similar to those presented earlier for Nb_3Sn. The role of possible excitons on the Raman spectra is examined. These theoretical results are then used to discuss the self-energy of a Raman-active optical phonon in a superconductor.

I. INTRODUCTION

At very low temperature the presence of the energy gap Δ in a superconductor prevents the conduction electrons from being excited unless the energy transferred exceeds 2Δ.[1] There should, therefore, be no electronic Raman scattering for energy transfers below 2Δ. Early calculations of the electronic Raman effect in superconductors neglected anisotropy in Δ and in the attractive electron-electron interaction, and were made in the limit of large wave-vector transfer q.[2-6] In a metal the relevant value of q is δ^{-1}, where δ is the optical penetration depth, and "large q" means that δ is small compared with the coherence length $\xi=\hbar v_F(2\Delta)^{-1}$, where v_F is the electron velocity at the Fermi surface. In this limit the calculations predicted that at zero temperature the scattered intensity would discontinuously turn on at 2Δ to a value above that of a normal metal, and for increasing energy transfer it would rise, but gradually approach the normal-metal value from above.[2-5] The first reported attempt to see structure near 2Δ in a Raman-type experiment was performed on Nb_3Sn.[7] Given the recent results to be discussed below, one can probably characterize this attempt as unsuccessful. The first clear evidence of Raman scattering by gap excitations was the observation of 2Δ peaks in $2H$-$NbSe_2$.[8-10] The small-q limit characterizes this layered compound, which also undergoes a phase transition to a charge-density-wave (CDW) state at a temperature above the superconducting transition temperature. Studies of the Raman spectrum in a magnetic field[8,9] and use of impurities to quench the CDW (Ref. 10) strongly suggested that the Raman peaks at 2Δ owed their Raman activity to coupling of the electronic excitations to Raman-active amplitude modes of the CDW. Two theories of this coupling have been published.[11,12]

The second clear case of evidence of Raman scattering from gap excitations was provided by simultaneous reports by two groups of the observations of peaks near 2Δ in Nb_3Sn and V_3Si.[13-17] The samples studied in most detail underwent a cubic-to-tetragonal martensitic transformation at temperatures above the superconducting transition temperature; nevertheless, it is convenient to describe the Raman symmetries as though the samples remained cubic. In a transforming sample of Nb_3Sn, peaks near 2Δ were seen in A_{1g}, E_g, and T_{2g} symmetries.[13-15] The E_g peak was about 20% lower in energy than the other two peaks.[13,15] In a nontransforming sample of V_3Si a peak was seen in E_g and A_{1g} symmetries, but the A_{1g} peak was too weak to analyze.[13,15] The temperature dependence of the E_g peak in transforming V_3Si was studied in some detail and the data were presented on the E_g peak in a nontransforming sample of Nb_3Sn by Hackl *et al.*[16,17] There is also some evidence of a 2Δ peak in Nb.[13]

Dierker *et al.* fitted their Nb_3Sn results with a theoretical expression derived using Bardeen-Cooper-Schrieffer (BCS) theory[1] in the limit $q\rightarrow 0$.[13-15] They assumed that the peaks near 2Δ were due to direct Raman scattering from quasiparticle pairs without the intervention of indirect coupling via phonons. This assumption appears justified (1) in the case of the 2Δ peak of A_{1g} symmetry by the absence of any Raman-active phonon of A_{1g} symmetry, (2) in the case of the 2Δ peak of T_{2g} symmetry by the weakness of the Raman scattering from the T_{2g} phonon, and (3) in the case of the 2Δ peak of E_g symmetry by the fact that the CDW-like E_g optical phonon in Nb_3Sn has a frequency of about $7\Delta/\hbar$, too far from $2\Delta/\hbar$ for strong admixing (whereas the CDW phonons in $2H$-$NbSe_2$ have frequencies of about $4\Delta/\hbar$). Dierker *et al.* attributed the lower value of the E_g gap peak frequency in Nb_3Sn to anisotropy of the gap Δ_k as a function of wave vector $\vec{k}$ on the Fermi surface combined with different weighting of the Δ_k's in the different Raman symmetries.

In the present paper we develop the theory in some detail for zero temperature using an anisotropic, nonretarded, attractive electron-electron interaction. We will correct the "bare" Raman matrix element for the effects of final-state interactions (vertex corrections), to make the theory gauge invariant, and we will correct for screening

of the vertex by the Coulomb interaction. In the $q\rightarrow 0$ limit either of these corrections essentially subtracts the Fermi-surface average of the Raman matrix element from that matrix element,[5] apart from small Fermi-liquid-like corrections.

In Sec. II we derive the Raman spectral function for a superconductor using results from second-order time-dependent perturbation theory. More attention is paid to the wave-vector dependence than is found in previous treatments.[2–6] Some details of the derivation and evaluation for finite q are given in Appendixes A and B. Derivations and numerical results for the Raman spectral function after integration over the component of q perpendicular to the interface, are presented elsewhere.[18]

Section III is devoted to the effect of vertex and Coulomb corrections. In addition, we examine the possibility that the observed E_g Raman peak in Nb_3Sn might be due to an "exciton" of that symmetry rather than gap anisotropy. In Sec. IV the results of Sec. III are applied to the polarization operator (self-energy) for an optical phonon. Results are summarized in Sec. V.

II. PERTURBATION THEORY

Electronic Raman scattering can be treated by considering the perturbation Hamiltonian

$$H'=\frac{1}{2m}\sum_j\left|\vec{p}_j-\frac{e}{c}\vec{A}(\vec{r}_j)\right|^2-\frac{1}{2m}\sum_j p_j^2\ , \tag{1a}$$

where $\vec{A}(\vec{r}_j)$ is the vector potential of the optical fields acting on the jth electron and $\vec{p}_j$ is that electron's momentum. The term in Eq. (1a) second order in A, used in the first order of perturbation theory, combines with the term first order in A used in the second order of perturbation theory. More precisely, the $\vec{p}_j\cdot\vec{A}(\vec{r}_j)$ term in Eq. (1a) induces transitions from the conduction-band states, denoted by $|k)$ to higher or lower band states $|bk)$ of energies ϵ_k and ϵ_{bk}, respectively. The photon scattering vertex is then given by the densitylike operator

$$\tilde{\rho}_{\vec{q}}=\sum_{\vec{k},\sigma} c^{\dagger}_{\vec{k}+\vec{q},\sigma}c_{\vec{k},\sigma}\gamma_{\vec{k}}\ , \tag{1b}$$

where[5]

$$\gamma_{\vec{k}}=(\vec{e}_i\cdot\vec{e}_s)+m^{-1}\sum_b\left[\frac{(k\mid\vec{p}\cdot\vec{e}_s\mid bk)(bk\mid\vec{p}\cdot\vec{e}_i\mid k)}{\epsilon_k-\epsilon_{bk}+\omega_i}+\frac{(k\mid\vec{p}\cdot\vec{e}_i\mid bk)(bk\mid\vec{p}\cdot\vec{e}_s\mid k)}{\epsilon_k-\epsilon_{bk}-\omega_s}\right], \tag{1c}$$

and where $c_{\vec{k},\sigma}$ is the annihilation operator for an electron of wave vector $\vec{k}$ and spin σ in the conduction band, and we use units in which $\hbar=1$. The quantities $\vec{e}_i$ and $\vec{e}_s$ denote polarization unit vectors for the incident and scattered photons.

The "internal" photon cross section per unit volume (which neglects reflection losses at the surface) is then given by

$$\frac{d^2R}{d\Omega\,d\omega}=r_o^2\tilde{S}(\vec{q},\omega)\ , \tag{1d}$$

where $r_o=e^2/mc^2$ is the Thomson radius, and where

$$\tilde{S}(\vec{q},\omega)=(2\pi)^{-1}\int_{-\infty}^{\infty}dt\exp(-i\omega t)\langle\tilde{\rho}_{\vec{q}}(0)\tilde{\rho}_{\vec{q}}(t)\rangle\ . \tag{1e}$$

$\tilde{S}(\vec{q},\omega)$ has been calculated for zero temperature for the BCS model of a superconductor by Abrikosov and Fal'kovskii,[2] and by Tong and Maradudin[3] with γ_k given by the first term of Eq. (1c). The use of the full Eq. (1c) can be accounted for in their result by inserting a factor of $|\gamma_k|^2/(\vec{e}_i\cdot\vec{e}_s)^2$ into the final sum over the wave vector, giving

$$\tilde{S}(\vec{q},\omega)=\int\frac{d^3k}{(2\pi)^3}\delta(\omega-E-E')\times\left[\frac{EE'-\epsilon_k\epsilon_k'+\Delta_k^2}{2EE'}\right]|\gamma_{\vec{k}}|^2\ . \tag{2a}$$

Here Δ_k is the gap parameter, assumed to be slowly varying near the Fermi surface, and $\epsilon_k'=\epsilon_{k+q}\approx\epsilon_k+\vec{q}\cdot\vec{v}_k$. The zero of energy for ϵ_k is assumed to be the Fermi energy. The quasiparticle energies E and E' obey

$$E=(\epsilon_k^2+\Delta_k^2)^{1/2}\ ,\quad E'=(\epsilon_{k'}^2+\Delta_{k'}^2)^{1/2}\ . \tag{2b}$$

The factor $(EE'-\epsilon_k\epsilon_{k'}+\Delta_k^2)/(2EE')$ in Eq. (2a) is the BCS coherence factor for a type-I excitation.

Equations (2a) and (2b) are rearranged in Appendix A to give

$$\tilde{S}(q,\omega)=4N(0)\omega^2\left\langle\frac{|\gamma_k|^2\Delta_k^2}{[\omega^2-(\vec{q}\cdot\vec{v}_k)^2]^{3/2}[\omega^2-(\vec{q}\cdot\vec{v}_k)^2-4\Delta_k^2]^{1/2}}\right\rangle_k', \tag{3a}$$

where $N(0)$ is the density of states for one spin, where for a function $F(k)$ we define a Fermi-surface average by

$$N(0)\langle F(k)\rangle_k'\equiv\int'\frac{d^3k}{(2\pi)^3}F(k)\delta(\epsilon_k)\ , \tag{3b}$$

and where the prime means that the integral in Eq. (3b) is restricted to those values of $\vec{k}$ such that

$$\omega^2>4\Delta_k^2+(\vec{q}\cdot\vec{v}_k)^2\ . \tag{3c}$$

We may evaluate Eq. (3c) further assuming a constant gap $\Delta_k=\Delta$, a constant scattering vertex $\gamma_k=\gamma$, and a spherical Fermi surface where $|\vec{v}_k|=v_F$ is a constant. This is done in Appendix B. Some numerical results for $\tilde{S}_{\rm red}(q,\omega)=\tilde{S}(q,\omega)[N(0)\gamma^2]^{-1}$ are plotted in Fig. 1.

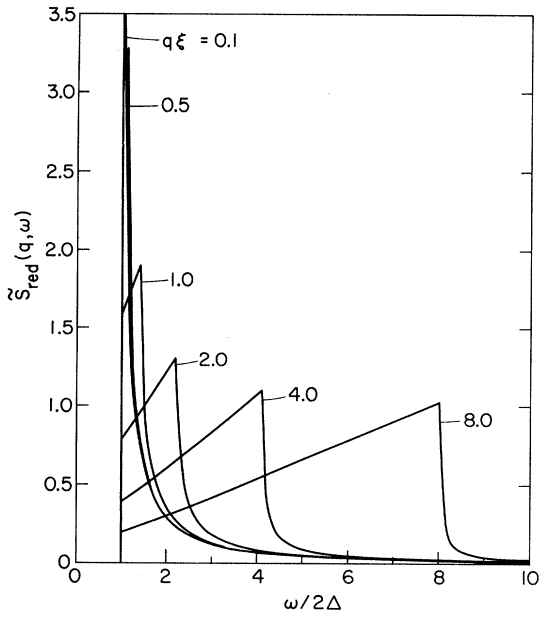

FIG. 1. Reduced structure factor $\tilde{S}_{\rm red}(q,\omega)=\tilde{S}(q,\omega)[N(0)\gamma^2]^{-1}$ vs $\omega/(2\Delta)$ for $q\xi=0.1$, 0.5, 1.0, 2.0, 4.0, and 8.0 where $\xi=v_F/2\Delta$ is the coherence length.

Actually, only $\vec{q}_{||}$, the component of $\vec{q}$ parallel to the interface, is well defined in a Raman experiment in metals.[19] The perpendicular component q_z has both real ($\equiv q_\perp$) and imaginary components ($\equiv\delta^{-1}$), where δ is the penetration depth for the incident optical intensity, and must be averaged over. The ratio of scattered to incident intensities is proportional to

$$I(\delta,q_\perp,q_{||},\omega)\equiv\pi^{-1}\int_{-\infty}^{\infty}\frac{dq_z}{(q_z+q_\perp)^2+\delta^{-2}}\times\tilde{S}(q=(q_z^2+q_{||}^2)^{1/2},\omega)\ . \tag{4a}$$

This result depends only on the magnitude $q_{||}$ of $\vec{q}_{||}$. Equation (4a) generally requires numerical evaluation; however, in certain cases analytical expressions can be found which semiquantitatively display the behavior of the function. This was done in detail in Ref. 18, and we display some results here.

In Figs. 2–4 we have plotted

$$I_{\rm red}(\delta,q_\perp,q_{||},\omega)\equiv\pi I(\delta,q_\perp,q_{||},\omega)[N(0)\gamma^2\delta]^{-1}$$

from (4a) versus $\omega/2\Delta$ in the near-gap region for the dimensionless ratio $r_o=0.1$–10.0, where

$$r_o\equiv\frac{\delta^{-1}v_F}{2\Delta}=\xi/\delta\ , \tag{4b}$$

and

$$\xi=v_F/2\Delta \tag{4c}$$

is the coherence length. We similarly define $r_\perp\equiv q_\perp\xi$ and $r_{||}\equiv q_{||}\xi$. The curves for $r_0\lesssim 0.1$ are equivalent to those for $r_o=0.1$. Figures 2, 3, and 4 correspond to $\eta\equiv(r_{||}^2+r_\perp^2)^{1/2}/r_0=0.1$, 0.5, and 2.0, respectively, while

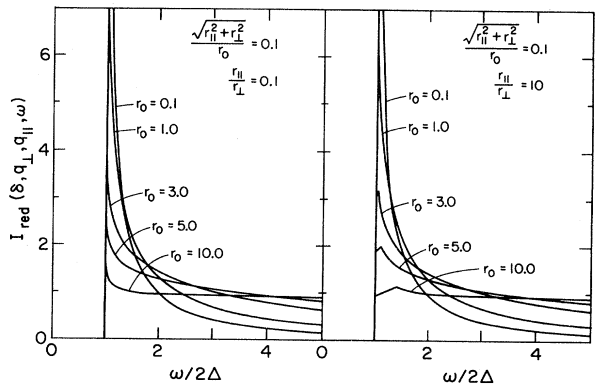

FIG. 2. $I_{\rm red}(\delta,q_\perp,q_{||},\omega)=\pi I(\delta,q_\perp,q_{||},\omega)[N(0)\gamma^2]^{-1}$ vs $\omega/2\Delta$.

the two panels of each figure correspond to $r_{||}/r_\perp=0.1$ and 10.0. Note that

$$\lim_{\substack{r_o\to 0\\ \eta\to 0}}\pi I(\delta,q_\perp,q_{||},\omega)/\delta=\tilde{S}(q=0,\omega)\ . \tag{4d}$$

This is a good approximation to I for $r_o\lesssim 1$ and $\eta\lesssim 1$; the main effect of finite $q_\perp$ and $q_{||}$ is to remove the singularity very near to $\omega=2\Delta$. For $r_o\gtrsim 1$ and $r_{||}\gg r_\perp$ the scattering near $\omega=2\Delta$ is strongly suppressed, the curves becoming rather featureless. For $r_o>1$ and $r_{||}\gg r_\perp$ a cusp appears at $\omega=2\Delta(1+r_{||}^2)^{1/2}$. The sharpness of this cusp is a result of our assumptions in Appendix B of a spherical Fermi surface, and it will be rounded for an anisotropic Fermi surface.

We feel that in the general case when $\Delta_k\neq$const and when $\gamma_k\neq$const, it will still be true that a good approximation to the frequency dependence of $\pi I(\delta,q_\perp,q_{||},\omega)$ will be given by $\delta\tilde{S}(q=0,\omega)$ with an appropriate weighting of Δ_k's , as long as the penetration depth is of order of or greater than the coherence length and $(q_{||}^2+q_\perp^2)^{1/2}\lesssim\delta^{-1}$.

As discussed earlier, experimental results now exist for Raman scattering by gap excitations in $2H$-$NbSe_2$,[8–10] Nb_3Sn,[13–17] V_3Si,[13–17] and Nb.[13] In Fig. 5 we have plotted $I_{\rm red}(\delta,q_\perp,q_{||},\omega)$ for each of these materials using the parameters ξ, r_o, $r_\perp$, and $r_{||}$ tabulated in Table I. The small r_o values for $2H$-$NbSe_2$, Nb_3Sn, and V_3Si make

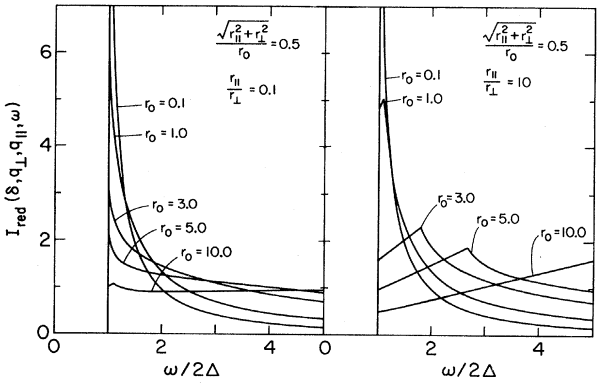

FIG. 3. $I_{\rm red}(\delta,q_\perp,q_{||},\omega)=\pi I(\delta,q_\perp,q_{||},\omega)[N(0)\gamma^2]^{-1}$ vs $\omega/2\Delta$.

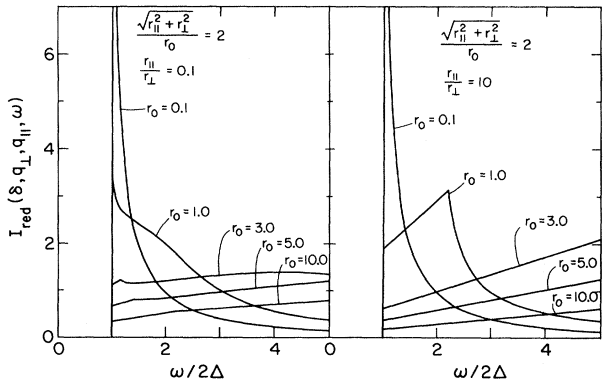

FIG. 4. $I_{\rm red}(\delta,q_\perp,q_{||},\omega)=\pi I(\delta,q_\perp,p_{||},\omega)[N(0)\gamma^2]^{-1}$ vs $\omega/2\Delta$.

$I_{\rm red}(\delta,q_\perp,q_{||},\omega)$ differ little from an inverse square-root singularity, as discussed in Ref. 18. Note the drastic effect of the large coherence length of niobium in reducing the scattering intensity at 2Δ compared to the other materials.

In Figs. 6 and 7 we show Raman spectra from a sample of V_3Si [$T_c=16.85$ K, the residual resistivity ratio (RRR) is 15, and $2\Delta\sim41$ cm^{-1}], which is not believed to undergo a martensitic transformation, taken at 1.8 and 40 K. The peaks near 45 cm^{-1} represent scattering from gap excitations. They appear in both E_g and A_{1g} symmetries. The smooth solid lines through the peaks are fits to the data based on Eq. (B5), convoluted with a Gaussian distribution of Δ in the manner of Eqs. (34f) and (34g) in order to mimic gap anisotropy, and then convoluted with a Gaussian to mimic the spectrometer response function. The fits clearly describe the data well; the results are given in Table II. Although the A_{1g} gap peak is too weak to isolate by subtraction as Dierker *et al.*[13,15] have done for Nb_3Sn, one can infer from the increase in Δ_0 in going from E_g to $A_{1g}+E_g$ to $A_{1g}+\frac{1}{4}E_g$ that the E_g gap peak frequency in V_3Si is $\gtrsim 10\%$ lower than the A_{1g} gap peak frequency.

Raman spectra from single-crystal, thin-film niobium ($T_c=9.3$ K, the RRR is 22.4, $2\Delta\sim25$ cm^{-1}, and thickness ≈2000 Å) are shown in Fig. 8. Note the extreme weakness of the scattering in the vicinity of 2Δ. This is consistent both with the prediction of Fig. 5 and with the relatively weaker Fermi-surface anisotropy of niobium compared to the $A15$ compounds Nb_3Sn and V_3Si.

TABLE I. Dimensionless real wave-vector transfers $r_\perp, r_{||}$ in $2H$-$NbSe_2$, Nb_3Sn, V_3Si, and Nb normalized by the coherence length ξ compared with the normalized imaginary wave vector r_o.

Sample	ξ (Å)	r_o	$r_\perp$	$r_{||}$
$2H$-$NbSe_2$	23[a]	0.114[d]	0.206	0.026
Nb_3Sn	73[b]	0.468[e]	0.313	0.084
V_3Si	87[b]	0.710[e]	0.465	0.010
Nb	450[c]	3.35[f]	3.05	0.513

[a]The value of ξ perpendicular to the layers is given. P. deTrey, S. Gygax, and J. P. Jan, J. Low Temp. Phys. 11, 421 (1973).
[b]T. P. Orlando, E. J. McNiff, S. Foner, and M. R. Beasley, Phys. Rev. B 19, 4545 (1979).
[c]G. W. Crabtree, D. H. Dye, D. B. Karin, and J. B. Ketterson, in *Superconductivity in d- and f-Band Metals*, edited by H. Suhl, and M. B. Maple (Academic, New York, 1980), p. 113.
[d]Optical constants from R. T. Harley and P. A. Fleury, J. Phys. C 12, L863 (1979).
[e]Optical constants from S. B. Dierker and M. V. Klein (unpublished).
[f]Optical constants from J. J. Carroll, S. T. Ceyer, and A. J. Melmed, J. Opt. Soc. Am. 72, 668 (1982).

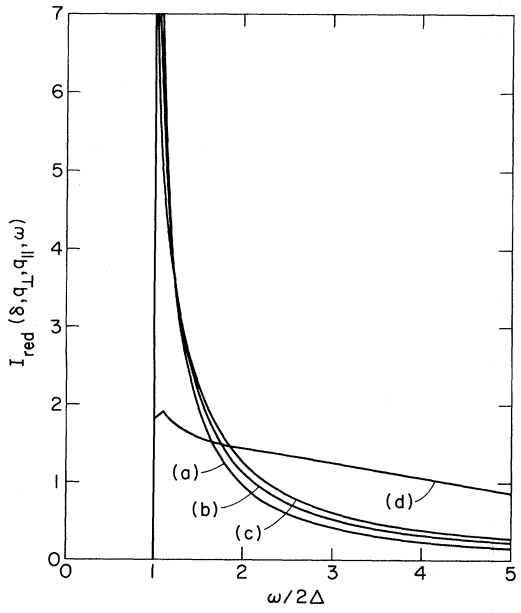

FIG. 5. $I_{\rm red}(\delta,q_\perp,q_{||},\omega)$ vs $\omega/2\Delta$ evaluated for the parameters (see Table I) appropriate for (a) $2H$-$NbSe_2$, (b) Nb_3Sn, (c) V_3Si, and (d) Nb.

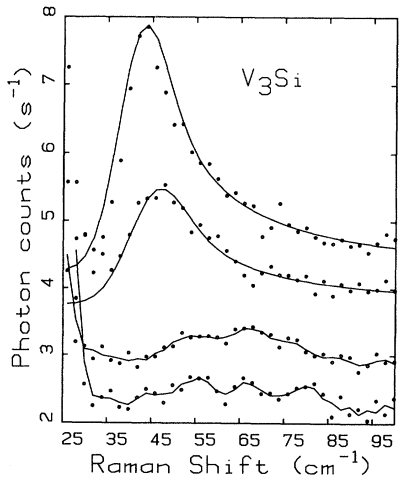

FIG. 6. Raman spectra of V_3Si. Lower two curves are at 40 K, and upper curves are at 1.8 K. Symmetries are as follows: top and bottom, $\frac{3}{4}E_g$; middle two, $A_{1g}+\frac{1}{4}E_g+T_{2g}$. Top curve has been shifted upward by 1.0 count/s, middle two curves by 0.5 count/s. Upper two smooth solid curves are theoretical fits, lower two solid curves are three point averages of the data.

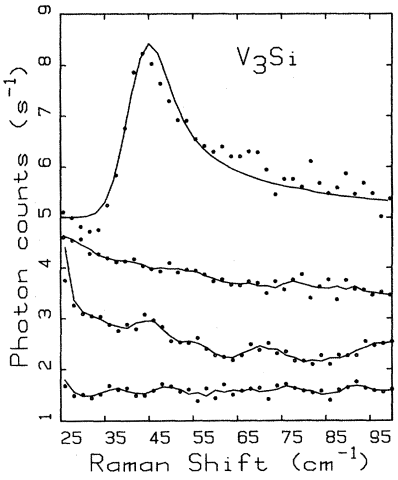

FIG. 7. Raman spectra of V_3Si. Lower two curves are at 40 K and upper curves are at 1.8 K. Symmetries are as follows: top and third from top, $A_{1g}+E_g$; bottom and third from bottom, T_{2g}. Top two curves have been shifted upward by 1.5 count/s. Top smooth-solid curve is a theoretical fit, lower three solid curves are three point averages of the data.

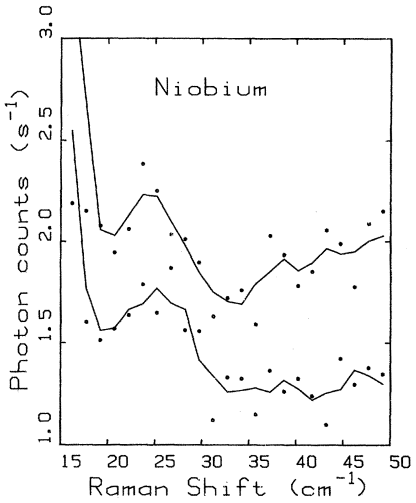

FIG. 8. Raman spectra of Nb at 1.8 K. Symmetries are as follows: top curve, $A_{1g}+\frac{4}{3}T_{2g}$; bottom curve, $2E_g+\frac{1}{3}T_{2g}$. Solid curves are three point averages of the data.

III. VERTEX AND POLARIZATION CORRECTIONS

A. Derivation

The results in Eqs. (2a), (3a), or (4a) apply to noninteracting pairs of BCS quasiparticles. We now take into account the interaction between the quasiparticles via the same attractive interaction responsible for superconductivity, and also include polarization corrections due to the long-range Coulomb interaction. We do this using Green's functions.[20,21] Intraband electronic Raman scattering involves the discontinuity in a four-vertex function F as the frequency variable $\omega=q_0$ crosses the real axis from above.[22] Figure 9 shows the four contributions to F for noninteracting electron-hole excitations in a normal metal. In a superconductor these become mixed with quasiparticle-pair excitations. The vertical lines b and b' refer to non-conduction-band Bloch states as introduced in connection with Eqs. (1b) and (1c). Electron-electron interactions with carriers in the conduction band will produce a finite width w_{bk} to Bloch state k in band b.[23]

1. *Bare vertices*

The vertex pair 1-2 may be treated as a single vertex, as may the vertex pair 3-4 (Fig. 10). Then, the F function has the character of a polarization "bubble." When the A^2 term from Eq. (1a) is included, the effective matrix element at vertex 1-2 is given by Eq. (1c) with ω_i replaced by ω_i+iw_{bk} and ω_s replaced by ω_s+iw_{bk}. The effective matrix element at vertex 3-4 is $\gamma'_k=\gamma_k^*$. The width w_{bk} will be typically $\frac{1}{3}$ eV or greater.[23] Hence, any changes in γ_k due to superconductivity can be neglected, and we can set $\omega_s=\omega_i$ with little error. If the photon energies are neglected with respect to the band gaps in the denominators of Eq. (1c), γ_k becomes simply $[m/m^*(k)]_{i,s}$, the scalar product of the reciprocal effective-mass tensor for wave vector $\vec{k}$ with $\vec{e}_i$ and $\vec{e}_s$.[5]

We use the Nambu spinor representation[21] that employs the matrices

$$\tau_0=\begin{bmatrix}1&0\\0&1\end{bmatrix},\quad \tau_1=\begin{bmatrix}0&1\\1&0\end{bmatrix},$$
$$\tau_2=i\begin{bmatrix}0&-1\\1&0\end{bmatrix},\quad \tau_3=\begin{bmatrix}1&0\\0&-1\end{bmatrix}. \tag{5}$$

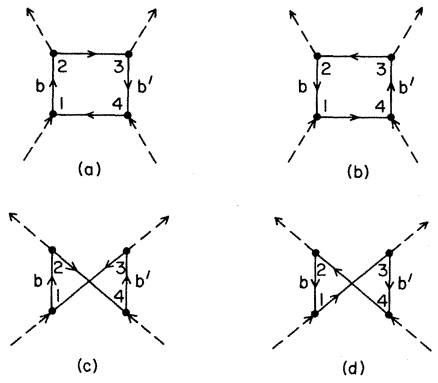

FIG. 9. The four-vertex diagrams for noninteracting electron-hole excitations in a normal metal. Solid lines refer to electrons or holes, dashed lines to photons. At vertices 1 and 4 the operator $(\vec{p}\cdot\vec{e}_i)$ acts, and at vertices 2 and 3 operator $(\vec{p}\cdot\vec{e}_s)$ acts. These four diagrams are to be supplemented by a diagram where vertices (1,2) and/or (3,4) are replaced by a single vertex where $(\vec{e}_i\cdot\vec{e}_s)\rho_q$ acts.

TABLE II. $\Delta_0\pm\sigma$ from fits to Raman data on V_3Si.

	$\Delta_0\pm\sigma$ (cm^{-1})
E_g	20.0±2.4
$A_{1g}+E_g$	21.2±1.8
$A_{1g}+\frac{1}{4}E_g$	21.5±2.8

FIG. 10. The effective vertices appearing in Fig. 3.

FIG. 11. Diagrammatic form of the integral equation, Eq. (6b).

The bare vertex γ_k now becomes the matrix

$$\underline{\gamma}(k)=\gamma_k\underline{\tau}_3 . \tag{6a}$$

2. *Interactions among particles; vertex functions*

Interactions between the quasiparticles are treated by using, instead of $\underline{\gamma}(k)$, the vertex function $\underline{\Gamma}(k_+,k_-)$, which obeys the vertex equation

$$\underline{\Gamma}(k_+,k_-)=\underline{\gamma}(k)+\int\frac{d^4k'}{(2\pi)^4 i}\underline{\tau}_3\underline{G}(k'_+)\underline{\Gamma}(k'_-,k'_+)\times\underline{G}(k'_-)\underline{\tau}_3 D(\vec{k},\vec{k}') . \tag{6b}$$

In Eq. (6b) we have used four-vector notation: $k=(\vec{k},k_0)$, $d^4k=d^3k\,d\vec{k}_0$, and $k_\pm=k\pm q/2$ with $q=(\vec{q},q_0=\omega)$, etc. The interaction is denoted by $D(\vec{k},\vec{k}')$. It will be assumed to be nonretarded. Equation (6b) is shown diagrammatically in Fig. 11.

The polarization bubble with a corrected vertex $\underline{\Gamma}$ on the left-hand side and a bare vertex $\underline{\gamma}'$ on the right-hand side will be denoted by $B_{\Gamma\gamma'}(q)$. It is given by (Fig. 12)

$$B_{\Gamma\gamma'}(q)=-\int\frac{d^4k}{(2\pi)^4 i}\mathrm{Tr}[\underline{G}(k_+)\underline{\Gamma}(k_+,k_-)\underline{G}(k_-)\underline{\tau}_3]\gamma'_k , \tag{6c}$$

where $\underline{\Gamma}$ satisfies Eq. (6b). The Raman intensity is obtained by generalizing $\tilde{S}(\vec{q},\omega)$ of Eqs. (1a)–(1e) to finite temperature, for intermediate-state damping, and for vertex effects using Kawabata's four-vertex function.[22] The generalization is given by

$$\tilde{S}(\vec{q},\omega)\to-[1+n(\omega)][B_{\Gamma\gamma^*}(\vec{q},\omega+i0^+)-B_{\Gamma\gamma^*}(\vec{q},\omega-i0^+)]/2\pi i , \tag{6d}$$

where $n(\omega)$ is the Bose function. Equation (6d) represents a generalization of the fluctuation-dissipation theorem for Raman scattering. We assume $T=0$, making it unnecessary to interpret the frequency variables in Eqs. (6b) and (6c) as Matsubara frequencies. Eventually, we shall replace $B_{\Gamma\gamma^*}$ by $B_{\Lambda\gamma^*}$ [see Eq. (21)]. Results for a nonretarded, factorizable interaction are given in Sec. III A 6.

The electronic Green's-function matrix appearing in Eqs. (6b) and (6c) is given by[21]

$$\underline{G}(k)=\frac{i(k_0\underline{\tau}_0+\epsilon_k\underline{\tau}_3+\Delta_k\underline{\tau}_1)}{k_0^2-\epsilon_k^2-\Delta_k^2} . \tag{7}$$

In writing $\underline{G}(k'\pm q/2)$, which will be used in (6b) or (6c), we approximate $\Delta_{k\pm q/2}$ by Δ_k and $\epsilon_{k'\pm 1/2q}$ by $\epsilon_{k'}\pm\frac{1}{2}\vec{q}\cdot\vec{v}_{k'}$. We note that the strong k' dependence of the integrands in Eqs. (6b) and (6c) results from the explicit dependence on $\epsilon_{k'}$, and treat it using the approximation of Eq. (A1) in Appendix A. The only components of $\underline{\Gamma}$ that are nonzero in the $\vec{q}=0$ limit are those proportional to $\underline{\tau}_3$ and to $\underline{\tau}_2$. We neglect the other component, which is proportional to $\underline{\tau}_0$, and write

$$\underline{\Gamma}(k_+,k_-)=\Gamma^{(3)}(\vec{k},\vec{q},\omega)\underline{\tau}_3+\Gamma^{(2)}(\vec{k},\vec{q},\omega)\underline{\tau}_2 . \tag{8}$$

3. *Results of performing k'_0 and ϵ' integrations*

Integrals of the type appearing in Eqs. (6b) and (6c) have been evaluated by Vaks *et al.*[24] The results are expressible using the function

$$f_k\equiv f(\beta_k)=\beta_k^{-1}(1-\beta_k^2)^{-1/2}\arcsin\beta_k , \tag{9a}$$

where

$$\beta_k^2=\frac{\omega^2-(\vec{q}\cdot\vec{v}_k)^2}{4\Delta_k^2} . \tag{9b}$$

Using their assumption of a k-independent cutoff frequency ω_c, we find

$$\Gamma^{(3)}(\vec{k},\vec{q},\omega)=\gamma_k-\int\frac{d^3k'}{(2\pi)^3}\delta(\epsilon_{k'})D(\vec{k},\vec{k}')\left[-\left[\frac{f_{k'}\omega^2-(\vec{q}\cdot\vec{v}_{\vec{k}'})^2}{\omega^2-(\vec{q}\cdot\vec{v}_{k'})^2}\right]\Gamma^{(3)}(\vec{k}',\vec{q},\omega)-\frac{i\omega f_{k'}}{2\Delta_{k'}}\Gamma^{(2)}(\vec{k}',\vec{q},\omega)\right] , \tag{10a}$$

$$\Gamma^{(2)}(\vec{k},\vec{q},\omega)=-\int\frac{d^3k'}{(2\pi)^3}\delta(\epsilon_{k'})D(\vec{k},\vec{k}')\left[\left[\ln\frac{\omega_c}{|\Delta_{k'}|}+\frac{\omega^2-(\vec{q}\cdot\vec{v}_{k'})^2}{4\Delta_{k'}^2}f_{k'}\right]\Gamma^{(2)}(\vec{k}'\vec{q},\omega)-\frac{i\omega f_{k'}}{2\Delta_{k'}}\Gamma^{(3)}(\vec{k}',\vec{q},\omega)\right] , \tag{10b}$$

$$B_{\Gamma\gamma'}(\vec{q},\omega)=2\int\frac{d^3k}{(2\pi)^3}\delta(\epsilon_k)\left[-\left[\frac{f_k\omega^2-(\vec{q}\cdot\vec{v}_k)^2}{\omega^2-(\vec{q}\cdot\vec{v}_k)^2}\right]\Gamma^{(3)}(\vec{k},\vec{q},\omega)-\frac{i\omega f_k}{2\Delta_k}\Gamma^{(2)}(\vec{k},\vec{q},\omega)\right]\gamma'_k . \tag{10c}$$

4. Coulomb interaction

We now add the Coulomb interaction with matrix element

$$V_q=\frac{4\pi e^2}{q^2}(k+q\,|\,e^{i\vec{q}\cdot\vec{r}}\,|\,k)\,. \tag{11a}$$

The intra-conduction-band matrix element obeys the estimate

$$(k+q\,|\,e^{i\vec{q}\cdot\vec{r}}\,|\,k)=1+\Theta(qa)^2\,, \tag{11b}$$

where a is an interatomic spacing. Interband matrix elements of $e^{i\vec{q}\cdot\vec{r}}$ are of order qa. Thus to lowest order in q we treat only intraband processes and use

$$V_q=4\pi e^2/q^2\,. \tag{11c}$$

The full vertex function $\underline{\Lambda}(k_+,k_0)$ obeys the equation (Fig. 13)

$$\underline{\Lambda}(k_+,k_-)=\underline{\gamma}(k)+\int\frac{d^4k'}{(2\pi)^4 i}\underline{\tau}_3\underline{G}(k'_+)\underline{\Lambda}(k'_+,k'_-)\underline{G}(k'_-)\underline{\tau}_3 D(\vec{k},\vec{k}')+V_q\underline{\tau}_3 i\int\frac{d^4k'}{(2\pi)^4}\mathrm{Tr}[\underline{\tau}_3\underline{G}(k'_+)\underline{\Lambda}(k'_+,k'_-)\underline{G}(k'_-)]\,. \tag{12}$$

We recognize the last integral in (12) as the polarization

$$B_{\Lambda 1}\equiv-\int\frac{d^4k}{(2\pi)^4 i}\mathrm{Tr}[\underline{G}(k_+)\underline{\Lambda}(k_+,k_-)\underline{G}(k_-)\underline{\tau}_3] \tag{13}$$

by comparing it with Eq. (6c), with $\gamma'_k=1$. As pointed out by Nambu,[21] Eq. (12) takes the same form as Eq. (6b) with the inhomogeneous term $\underline{\gamma}(k)$ replaced by $\underline{\gamma}(k)+V_qB_{\Lambda 1}\underline{\tau}_3$.

The solution of Eq. (12) is

$$\underline{\Lambda}=\underline{\Gamma}+V_qB_{\Lambda 1}\underline{\Gamma}(1)\,, \tag{14}$$

where $\underline{\Gamma}(1)$ is the solution of Eq. (6b) with $\underline{\gamma}(k)=\underline{\tau}_3$. Hence the polarization $B_{\Lambda 1}$ obeys

$$B_{\Lambda 1}=B_{\Gamma 1}+V_qB_{\Lambda 1}B_{\Gamma(1)1}=\frac{B_{\Gamma 1}}{1-V_qB_{\Gamma(1)1}}=\frac{B_{\Gamma 1}}{\epsilon(q,\omega)}\,, \tag{15}$$

where $B_{\Gamma 1}$ is given by Eq. (6c) with $\gamma'_k=1$, and where $B_{\Gamma(1)1}$ is given by Eq. (6c) with $\gamma'_k=1$ and with use of $\underline{\Gamma}(1)$. The dielectric constant in Eq. (15) is

$$\epsilon(q,\omega)=1-\frac{4\pi e^2}{q^2}B_{\Gamma(1)1}\,. \tag{16}$$

The polarization we want is $B_{\Lambda\gamma^*}$, which from Eq. (14) is given by

$$\begin{aligned}B_{\Lambda\gamma^*}&=B_{\Gamma\gamma^*}+V_qB_{\Lambda 1}B_{\Gamma(1)\gamma^*}\\&=B_{\Gamma\gamma^*}+B_{\Gamma 1}V_qB_{\Gamma(1)\gamma^*}/\epsilon(q,\omega)\\&=B_{\Gamma\gamma^*}-\frac{B_{\Gamma 1}B_{\Gamma(1)\gamma^*}}{B_{\Gamma(1)1}-q^2/(4\pi e^2)}\,.\end{aligned} \tag{17}$$

The gap equation is obtained from Eq. (10b) by setting q,ω equal to zero and $\Gamma_2=\Delta_k$,

$$\Delta_k=-\int\frac{d^3k'}{(2\pi)^3}\delta(\epsilon_{k'})D(\vec{k},\vec{k}')\left[\ln\frac{\omega_c}{|\Delta_{k'}|}\right]\Delta_{k'}\,. \tag{18}$$

5. Expansion in Fermi-surface harmonics

We assume that $D(k,k')$ may be written as a sum of separable terms,

$$D(\vec{k},\vec{k}')=-\sum_L V_L e_L(\vec{k})e_L(\vec{k}')\,, \tag{19a}$$

where the $e_L(\vec{k})$ are "Fermi-surface harmonics,"[25] orthonormal on the Fermi surface,

$$\langle e_Le_{L'}\rangle=\delta_{LL'}\,. \tag{19b}$$

The notation $\langle F\rangle$ in Eq. (19b) denotes the Fermi-surface average of a function F_k,

$$\begin{aligned}\langle F\rangle=\langle F_k\rangle&=N(0)^{-1}\sum_k\delta(\epsilon_k)F_k\\&=N(0)^{-1}\int\frac{d^3k}{(2\pi)^3}\delta(\epsilon_k)F_k\,.\end{aligned} \tag{19c}$$

We anticipate the dominance in Eq. (19a) of the $L=0$ term, where $e_0(\vec{k})$ has the full factor-group symmetry (A_1) under rotations of $\vec{k}$ and is nodeless on the Fermi surface. We assume that V_0 is positive and larger than any other $|V_L|$. Neglecting admixtures of e_L with $L\neq 0$ produced by the logarithm in Eq. (18), we find that the

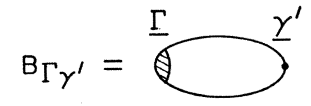

FIG. 12. Polarization bubble, Eq. (6c).

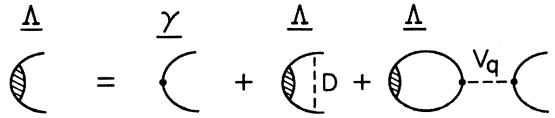

FIG. 13. Diagrammatic form of the integral equation, Eq. (12).

solution of (18) with the largest $|\Delta_k|$ is

$$\Delta_k = \Delta e_0(k) , \tag{20a}$$

where

$$\Delta = \langle \Delta_k^2 \rangle^{1/2} \tag{20b}$$

obeys the equation

$$1 = G_0[\ln(\omega_c/\Delta) - \langle (\ln e_0) e_0^2 \rangle] , \tag{20c}$$

where

$$G_0 \equiv N(0) V_0 . \tag{20d}$$

To solve Eqs. (10a) and (10b) we make the expansions

$$\Gamma^{(3)}(\vec{k},\vec{q},\omega) = \gamma_k + \sum_L \Gamma_L^{(3)} e_L(\vec{k}) , \tag{21a}$$

$$\Gamma^{(2)}(\vec{k},\vec{q},\omega) = \sum_L \Gamma_L^{(2)} e_L(\vec{k}) , \tag{21b}$$

where $\Gamma_L^{(3)}$ and $\Gamma_L^{(2)}$ are still functions of $\vec{q}$ and ω. Equation (10c) then gives

$$B_{\Gamma\gamma'} = B_{\Gamma\gamma'}(q,\omega) = -2N(0)\langle \gamma Q \gamma' \rangle - 2N(0) \sum_L \Gamma_L^{(3)} \langle e_L Q \gamma' \rangle - 2N(0)(i\omega/2\Delta) \sum_L \Gamma_L^{(2)} \langle e_L f \gamma'/e_0 \rangle , \tag{22a}$$

where

$$Q = Q_k(\vec{q},\omega) \equiv \frac{f_k \omega^2 - (\vec{q}\cdot\vec{v}_k)^2}{\omega^2 - (\vec{q}\cdot\vec{v}_k)^2} . \tag{22b}$$

Introducing

$$G_L \equiv N(0) V_L , \tag{23a}$$

we rewrite Eq. (10a) as

$$-G_L^{-1}\Gamma_L^{(3)} = \langle \gamma Q e_L \rangle + i\omega/(2\Delta) \sum_{L'} \Gamma_{L'}^{(2)} \langle f e_{L'} e_L/e_0 \rangle + \sum_{L'} \Gamma_{L'}^{(3)} \langle Q e_{L'} e_L \rangle \tag{23b}$$

and Eq. (10b) as

$$G_L^{-1}\Gamma_L^{(2)} = \sum_{L'} \Gamma_{L'}^{(2)} \langle \{\ln[\omega_c/(\Delta e_0)] + [\omega^2 - (\vec{q}\cdot\vec{v})^2] f/(4\Delta^2 e_0^2)\} e_L e_{L'} \rangle - (i\omega/2\Delta)\langle f\gamma e_L/e_0 \rangle - (i\omega/2\Delta) \sum_{L'} \Gamma_{L'}^{(3)} \langle f e_{L'} e_L/e_0 \rangle . \tag{23c}$$

The most important contribution to Eqs. (22), (23b), and (23bc) comes from the $L=0$ and $L'=0$ terms. We initially restrict ourselves to just such terms by writing ($V \equiv V_0$)

$$D(\vec{k},\vec{k}') = -V e_0(\vec{k}) e_0(\vec{k}') . \tag{24a}$$

With $e_0(\vec{k}) \neq$ const, this amounts to an anisotropic BCS model. We continue to assume that $e_0(\vec{k})$ is nodeless on the Fermi surface and has full factor-group symmetry under symmetry operations on $\vec{k}$. The vertex functions take the simple forms

$$\Gamma^{(3)}(\vec{k},\vec{q},\omega) = \gamma_k + \Gamma_0^{(3)} e_0(\vec{k}) , \tag{24b}$$

$$\Gamma^{(2)}(\vec{k},\vec{q},\omega) = \Gamma_0^{(2)} e_0(\vec{k}) . \tag{24c}$$

6. *Solutions*

The anisotropic BCS model, with interaction given by Eq. (24a), has been shown above to lead to solvable equations (23b) and (23c) for the vertex function. That function may be written in the matrix form [Eqs. (5), (8), (21a), and (21b)]

$$\underline{\Gamma}(k_+,k_-) = [\gamma_k + \Gamma_0^{(3)} e_0(\vec{k})]\underline{\tau}_3 + \Gamma_0^{(2)} e_0(\vec{k})\underline{\tau}_2 .$$

The solutions for the coefficients $\Gamma_0^{(3)}$ and $\Gamma_0^{(2)}$ are

$$\Gamma_0^{(3)} = \frac{-N(0)VA(\gamma e_0)}{1+N(0)VA(e_0^2)} , \tag{25a}$$

where an abbreviated notation has been introduced for the following average of functions g_k and h_k:

$$A(gh) \equiv \langle Qgh \rangle - \frac{\langle fg \rangle \langle fh \rangle}{\langle [1-(\vec{q}\cdot\vec{v}/\omega)^2] f \rangle} \tag{25b}$$

and

$$\frac{i\omega\Gamma_0^{(2)}}{2\Delta} = \frac{-\langle f\gamma \rangle - \Gamma_0^{(3)} \langle f e_0 \rangle}{\langle [1-(\vec{q}\cdot\vec{v}/\omega)^2] f \rangle} . \tag{25c}$$

The functions $f = f_k$ and $Q = Q_k$ are defined in Eqs. (9) and (22b), respectively. We then find from Eqs. (22a) and (25) that the polarization originally defined in Eq. (6c) obeys

$$B_{\Gamma\gamma'} = -2N(0)\left[A(\gamma,\gamma') - \frac{N(0)VA(\gamma e_0)A(\gamma' e_0)}{1+N(0)VA(e_0^2)}\right] . \tag{26}$$

We shall neglect the second term of Eq. (26). It produces Fermi-liquid-like corrections to the first term, but does not add any qualitatively new effects. Thus we write

$$B_{\Gamma\gamma'} = -2N(0)[\langle Q\gamma\gamma' \rangle - \langle f\gamma \rangle \langle f\gamma' \rangle / \langle P \rangle] , \tag{27a}$$

where

$$P = P_k(\vec{q},\omega) = f_k[1-(\vec{q}\cdot\vec{v}_k/\omega)^2] . \tag{27b}$$

Equation (17) then gives for the Coulomb-corrected polarization

$$B_{\Lambda\gamma^*}=-2N(0)\left[[\langle Q\,|\,\gamma\,|^2\rangle-\langle f\gamma\rangle\langle f\gamma^*\rangle/\langle P\rangle]-\frac{[\langle Q\gamma\rangle-\langle f\gamma\rangle\langle f\rangle/\langle P\rangle][\langle Q\gamma^*\rangle-\langle f\gamma^*\rangle\langle f\rangle/\langle P\rangle]}{[\langle Q\rangle-\langle f\rangle^2/\langle P\rangle]+q^2/q_{\rm FT}^2}\right], \tag{28a}$$

where

$$q_{\rm FT}^2=8\pi N(0)e^2 \tag{28b}$$

is the square of the Fermi-Thomas (FT) wave vector. We expect $q_{\rm FT}a\gtrsim 1$, where a is a nearest-neighbor spacing. In most of what follows we shall neglect the q^2 term in the denominator of Eq. (28a) since the other terms in the denominator will usually be of order unity.

If the q^2 term in the denominator of Eq. (28a) is neglected, $B_{\Lambda\gamma^*}$ vanishes if $\gamma_k=$const. This is a consequence of the Coulomb polarization correction, which completely screens the effect of $\langle\gamma\rangle$ in $B_{\Gamma\gamma^*}$.[5,22] Thus if we write

$$\gamma_k=\delta\gamma_k+\langle\gamma\rangle\ , \tag{28c}$$

we obtain, from Eq. (28a),

$$B_{\Lambda\gamma^*}=-2N(0)\left[[\langle Q\,|\,\delta\gamma\,|^2\rangle-\langle f\delta\gamma\rangle\langle f\delta\gamma^*\rangle/\langle P\rangle]-\frac{[\langle Q\delta\gamma\rangle-\langle f\delta\gamma\rangle\langle f\rangle/\langle P\rangle][\langle Q\delta\gamma^*\rangle-\langle f\delta\gamma^*\rangle\langle f\rangle/\langle P\rangle]}{[\langle Q\rangle-\langle f\rangle^2/\langle P\rangle]}\right]. \tag{28d}$$

Each factor in square brackets in Eq. (28d) has a pole at the zero of $\langle P\rangle$, but that pole is actually removed, because Eq. (28d) can be rearranged into

$$B_{\Lambda\gamma^*}=-2N(0)\langle Q\,|\,\delta\gamma\,|^2\rangle+\frac{2N(0)}{\langle Q\rangle\langle P\rangle-\langle f\rangle^2}[\langle\delta\gamma Q\rangle\langle\delta\gamma^*Q\rangle\langle P\rangle+\langle Q\rangle\langle f\delta\gamma\rangle\langle f\delta\gamma^*\rangle$$
$$-\langle\delta\gamma Q\rangle\langle\delta\gamma^*f\rangle\langle f\rangle-\langle\delta\gamma^*Q\rangle\langle\delta\gamma f\rangle\langle f\rangle]\ . \tag{29}$$

This removable pole is that of the well-known Bogoliubov-Anderson collective mode,[26,27] for when β_k^2 is much less than unity, we obtain from Eqs. (9a) and (27b), assuming cubic symmetry,

$$0=\langle P\rangle=1-q^2v_F^2/3\omega^2\ ,$$

where

$$v_F^2=\langle v_k^2\rangle\ .$$

As is well known, the Coulomb corrections have removed this pole. One can show by keeping the q^2 term in the denominator of Eq. (17) that the pole has been pushed up to the plasma frequency. [See Eq. (32a).[21]]

B. Simplifications and discussion

1. *Leading approximation*

If we approximate $B_{\Lambda\gamma^*}$ by the first term of Eq. (28d) or Eq. (29), we obtain for the zero-temperature generalization of $\tilde{S}(\vec{q},\omega)$, as expressed by Eq. (6d),

$$\tilde{S}(\vec{q},\omega)=2N(0)\pi^{-1}\left\langle\frac{\omega^2}{\omega^2-(\vec{q}\cdot\vec{v}_k)^2}\,|\,\delta\gamma_k\,|^2{\rm Im}f(\beta_k+i0^+)\right\rangle_k$$
$$=4N(0)\omega^2\left\langle\frac{|\,\delta\gamma_k\,|^2\Delta_k^2}{[\omega^2-(\vec{q}\cdot\vec{v}_k)^2]^{3/2}[\omega^2-(\vec{q}\cdot\vec{v}_k)^2-4\Delta_k^2]^{1/2}}\right\rangle_k'\ . \tag{30}$$

We note that Eq. (30) is Eq. (3a) with γ_k replaced by $\delta\gamma_k$. $\tilde{S}(\vec{q},\omega)$ can also be written in the form of Eq. (A10e) with γ_k replaced by $\delta\gamma_k$. The remaining terms in Eq. (28d) or (29) contain factors such as $\langle f_k\delta\gamma_k\rangle$ or $\langle Q_k\delta\gamma_k\rangle$. Since $\langle\delta\gamma_k\rangle=0$, such factors will be nonzero only to the extent that the fluctuations $\delta\gamma_k$ are correlated with the k dependence of f_k or Q_k. These in turn occur via the k dependence of Δ_k and, for finite q, via the k dependence in $(\vec{q}\cdot\vec{v}_k)^2$. It is difficult to draw any general conclusions about the role of these factors in the generalization of $\tilde{S}(\vec{q},\omega)$. One hopes, of course, that they can be neglected. We now discuss three special cases in more detail.

2. *Normal metal*

The first case is that of a *normal metal.* Letting $\Delta_k\to 0$, we see from Eq. (9b) that $\beta_k^2\to\pm\infty$. By Eq. (9a) we have $f_k\to 0$. By Eq. (27a) we then find with

$$Q_k(\vec{q},\omega)=-(\vec{q}\cdot\vec{v}_k)^2/[\omega^2-(\vec{q}\cdot\vec{v}_k)^2]\ , \tag{31a}$$

$$B_{\Gamma\gamma'}=B_{\gamma\gamma'}=2N(0)\left\langle\frac{\gamma_k\gamma'_k(\vec{q}\cdot\vec{v}_k)^2}{\omega^2-(\vec{q}\cdot\vec{v}_k)^2}\right\rangle .$$

Note that no vertex corrections appear in Eq. (31a). Use of Eq. (17) with the q^2 term in the denominator dropped leads to the result

$$B_{\Lambda\gamma^*}=2N(0)\left\langle\frac{(\vec{q}\cdot\vec{v})^2\delta\tilde{\gamma}\delta\tilde{\gamma}^*}{\omega^2-(\vec{q}\cdot\vec{v})^2}\right\rangle , \tag{31b}$$

where

$$\delta\tilde{\gamma}_k\equiv\delta\gamma_k-\left\langle\frac{(\vec{q}\cdot\vec{v})^2\delta\gamma}{\omega^2-(\vec{q}\cdot\vec{v})^2}\right\rangle\left\langle\frac{(\vec{q}\cdot\vec{v})^2}{\omega^2-(\vec{q}\cdot\vec{v})^2}\right\rangle^{-1} , \tag{31c}$$

with a similar expression for $\delta\tilde{\gamma}_{k^*}$. Equation (31b) suggests that $B_{\Lambda\gamma^*}$ vanishes in the small-q limit where $(qv_F)^2\ll\omega^2$.

3. *Low frequencies*

The second case to be considered is $\omega\sim qv_F\ll 2\Delta$. Then, Eqs. (9a) and (9b) give $f_k\approx 1$, and Eq. (22b) gives $Q_k\approx 1$. The Coulomb-corrected polarization is, from Eq (28) after some rearranging,

$$B_{\Lambda\gamma^*}=-2N(0)\langle\,|\,\delta\gamma\,|^2\rangle+\frac{2N(0)\,|\,\langle\gamma\rangle\,|^2q^2v_F^2/3}{\omega^2-1/3q^2v_F^2-\omega_p^2} , \tag{32a}$$

where

$$\omega_p^2=8\pi N(0)e^2v_F^2/3 \tag{32b}$$

is the square of the plasma frequency. Equation (32a) gives no imaginary part to $B_{\Lambda\gamma^*}$ at low frequencies where it is valid.

4. *Frequencies close to the gap; symmetry arguments*

The third case occurs when $\omega\gtrsim 2\Delta\gg qv_F$. This $q\approx 0$ limit is the one of most interest, since, according to the discussion at the end of Sec. II, it should be valid when $\delta\gtrsim\xi$ and $\delta^{-1}\gtrsim(q_{\|}^2+q_{\perp}^2)^{1/2}$. Then $Q_k\approx f_k$, and we may neglect the q dependence of f_k. Equation (27a) then gives

$$\begin{aligned}B_{\Gamma\gamma'}&=-2N(0)[\langle f\gamma\gamma'\rangle-\langle f\gamma\rangle\langle f\gamma'\rangle/\langle f\rangle]\\&=-2N(0)[\langle f\delta\gamma\delta\gamma'\rangle-\langle f\delta\gamma\rangle\langle f\delta\gamma'\rangle/\langle f\rangle] .\end{aligned} \tag{33}$$

The Coulomb polarization correction of Eq. (17) gives

$$B_{\Lambda\gamma^*}=B_{\Gamma\gamma^*} ,$$

since for the Coulomb vertex, $\delta\gamma=0$. Thus the polarization we want obeys

$$\begin{aligned}B_{\Lambda\gamma^*}=B_{\Gamma\gamma^*}=-2N(0)[&\langle f\,|\,\delta\gamma\,|^2\rangle\\&-\langle f\delta\gamma\rangle\langle f\delta\gamma^*\rangle/\langle f\rangle] .\end{aligned} \tag{34a}$$

Since the gap Δ_k is an even function of k, f_k is also even in this limit of $q=0$. Thus only the even k parts of $\delta\gamma_k$ and $\delta\gamma_{k^*}$ are needed in the second term of Eq. (34a). If we separate γ_k as given by Eq. (1c) with width w_{bk} added into a sum of parts symmetric γ_k^s and antisymmetric γ_k^u under interchange of polarization vectors $\vec{e}_i$ and $\vec{e}_s$, where

$$\gamma_k^s=(\vec{e}_i\cdot\vec{e}_s)+\sum_b\frac{[(k\,|\,p_s\,|\,bk)(bk\,|\,p_i\,|\,k)+(k\,|\,p_i\,|\,bk)(bk\,|\,p_s\,|\,k)](\epsilon_k-\epsilon_{bk})}{m[(\epsilon-\epsilon_{bk})^2-(\omega_i+iw_{bk})^2]} \tag{34b}$$

and

$$\gamma_k^u=\sum_b\frac{[(k\,|\,p_i\,|\,bk)(bk\,|\,p_s\,|\,k)-(k\,|\,p_s\,|\,bk)(bk\,|\,p_i\,|\,k)](\omega_i+iw_{bk})}{m[(\epsilon_k-\epsilon_{bk})^2-(\omega_i+iw_{bk})^2]} , \tag{34c}$$

then it is easy to see that under the usual assumption that $|\,k)^*=|\,-k)$, etc., that γ_k^s is even and γ_k^u is odd under inversion in k space. We note that

$$\langle\gamma_k^u\rangle=\langle f_k\gamma_k^u\rangle=0 ,$$

and that

$$\langle f_k\delta\gamma_k^s\rangle=\langle f_k\delta\gamma_k^A\rangle ,$$

where $\delta\gamma_k^A$ is the part of $\delta\gamma_k^s$ that is fully symmetric under factor-group operations on k. This allows us to write Eq. (34a) in the form

$$\begin{aligned}B_{\Lambda\gamma}=B_{\Gamma\gamma^*}=-2N(0)(&\langle f_k[\,|\,\delta\gamma_k^s\,|^2+|\,\delta\gamma_k^u\,|^2]\rangle\\&-\langle f\delta\gamma^A\rangle\langle f\delta\gamma^{A*}\rangle/\langle f\rangle) .\end{aligned} \tag{34d}$$

If we further express $\delta\gamma_k$ as a sum of irreducible tensor components $\delta\gamma_k^{\Gamma}$ with respect to the indices i and s, we may write Eq. (34d) as

$$\begin{aligned}B_{\Lambda\gamma^*}=B_{\Gamma\gamma^*}=-2N(0)[&\langle f\,|\,\delta\gamma^A\,|^2\rangle\\&-\langle f\delta\gamma^A\rangle\langle f\delta\gamma^{A*}\rangle/\langle f\rangle]\\&-2N(0)\sum_{\Gamma\neq A}\langle f\,|\,\delta\gamma^{\Gamma}\,|^2\rangle .\end{aligned} \tag{34e}$$

Thus no irreducible components except the fully symmetric one require corrections. The importance of the second term in Eq. (34e) is not expected to be large. If we neglect that term, then Eq. (6d) gives

$$\tilde{S}(q\to 0,\omega)=\frac{4N(0)}{\omega}\sum_{\Gamma}\int_0^{\omega/2}\frac{\Delta^2P_{\Gamma}(\Delta)d\Delta}{(\omega^2-4\Delta^2)^{1/2}} , \tag{34f}$$

where

$$P_{\Gamma}(\Delta)=\langle\,|\,\delta\gamma_k^{\Gamma}\,|^2\delta(\Delta_k-\Delta)\rangle \tag{34g}$$

is a symmetry-weighted distribution function for the gap. Dierker *et al.* used Eqs. (34f) and (34g) to fit their data on Nb_3Sn and V_3Si with the use of Gaussians to model $P_\Gamma(\Delta)$ for $\Gamma=A_{1g}$, E_g, and T_{2g}.[15] The data and theoretical fits for V_3Si are shown in Figs. 6 and 7.

Another case of interest, namely, $qv_f \gg \omega \gtrsim 2\Delta$, has already been discussed by Abrikosov and Genkin,[5] who used an expression equivalent to Eq. (30). The important contributions come from bands on the Fermi surface where $\vec{v}_k \cdot \vec{q} \approx 0$. Integration on the Fermi surface in the direction perpendicular to the bands gives a contribution similar to Eq. (B2) in Appendix B. This must then be integrated along the bands.

C. Excitons

The notion of an exciton in a superconductor refers to the bound state of quasiparticle pairs at an energy of less than 2Δ.[28,29] If the attractive interaction is of the anisotropic BCS type given by Eq. (24a), the only such exciton is the Bogoliubov-Anderson collective mode, and the Coulomb correction eliminates that from influencing the low-frequency response. With the more general, attractive interaction of Eq. (19a) the presence of each extra term $-V_L e_L(\vec{k}) e_L(\vec{k}')$ for $L\neq 0$ gives a new exciton state. We now investigate the importance of such states for Raman scattering and argue that they are probably unimportant.

The general task of solving Eqs. (23b) and (23c) for $\Gamma_L^{(2)}$ and $\Gamma_L^{(3)}$ to be used in Eq. (22a) is greatly complicated by the coupling terms having $L\neq L'$. Such coupling is reduced if we go to the $q=0$ limit, which we do now. We expand

$$\gamma_k = \langle\gamma\rangle + \delta\gamma_k^A + \sum_{L\neq 0} \langle \gamma e_L\rangle e_L(k) \, . \tag{35}$$

We further assume that the $L\neq 0$ terms of Eqs. (19a) and (35) involve Fermi-surface harmonics $e_L(k)$ which are non-s-like (i.e., orthogonal to A_{1g}). Thus exciton effects will modify the last term in Eq. (34e). We assume that not only

$$\langle e_0 e_L\rangle = 0 \, , \tag{36a}$$

but also

$$\langle f e_L\rangle = 0 \, , \quad \langle f e_0 e_L\rangle = 0 \, , \quad \langle f e_L / e_0\rangle = 0 \, . \tag{36b}$$

We further assume, for $L\neq L'$ with L and $L'\neq 0$, that not only

$$\langle e_L e_{L'}\rangle = 0 \, , \tag{37a}$$

but also

$$\langle f e_L e_{L'}/e_0\rangle = 0 \, , \quad \langle f e_L e_{L'}\rangle = 0 \, , \quad \langle f e_L e_{L'}/e_0^2\rangle = 0 \, . \tag{37b}$$

The sums over L' on the right-hand side of Eqs. (23b) and (23c) then involve only $L'=L$, and those equations may readily be solved for $\Gamma_L^{(2)}$ and $\Gamma_L^{(3)}$. Equations (22a) and (34e) then give

$$B_{\Gamma\gamma^*} = -2N(0)[\langle f \,|\, \delta\gamma^A \,|^2\rangle - \langle f\delta\gamma^A\rangle\langle f\delta\gamma^{A*}\rangle/\langle f\rangle] - 2N(0) \sum_{L\neq 0} |\langle \gamma e_L\rangle|^2 \left[\frac{\langle f e_L^2\rangle - G_L g_L(\omega^2/4\Delta^2)[\langle f e_L^2/e_0^2\rangle\langle f e_L^2\rangle - \langle f e_L^2/e_0\rangle^2]}{1+\langle f e_L^2\rangle G_L - g_L \frac{\omega^2}{4\Delta^2}\langle f e_L^2/e_0^2\rangle - G_L g_L \frac{\omega^2}{4\Delta^2}[\langle f e_L^2/e^{0^2}\rangle\langle f e_L^2\rangle - \langle f e_L^2/e_0\rangle^2]} \right] , \tag{38a}$$

where

$$g_L \equiv G_L G_0/(G_0 - G_L) \, . \tag{38b}$$

When G_L (and g_L) equal zero, the expression in large parentheses in Eq. (38a) simplifies to $\langle f e_L^2\rangle$, and Eq. (38a) becomes consistent with Eqs. (34f) and (34g) if we identify the irreducible representation $\Gamma\neq A$ with the Fermi-surface harmonic $L\neq 0$ and note that

$$P_\Gamma(\Delta) \equiv P_L(\Delta) = |\langle \gamma e_L\rangle|^2 \langle e_L(k)^2 \delta(\Delta_k - \Delta)\rangle \, . \tag{38c}$$

For an isotropic gap, we have $e_0(k)=1$ and an f which is independent of k. Equation (38a) then simplifies to

$$B_{A\gamma^*} = B_{\Gamma\gamma^*} = -2N(0) f \langle \,|\, \delta\gamma^A \,|^2\rangle - 2N(0) \sum_{L\neq 0} \frac{|\langle \gamma e_L\rangle|^2 f}{1 - f[\omega^2 g_L/(4\Delta^2) - G_L]} \, . \tag{39}$$

The Lth term in Eq. (39) has a pole at $\omega_L < 2\Delta$, corresponding to an exciton of symmetry $e_L(k)$ when

$$\beta_L^2 g_L - G_L = (f_L)^{-1} \, , \tag{40}$$

where $f_L \equiv f(\beta_L)$ and where $\beta_L = \omega_L/(2\Delta)$. Equation (40) is equivalent to Eq. (4.7) of Bardassis and Schrieffer.[28]

We obtain for the spectrum the result

$$-\mathrm{Im} B_{A\gamma^*} = 2N(0) \sum_{L\neq 0} |\langle \gamma e_L\rangle|^2 \left[(2\Delta)\pi S_L \delta(\omega - \omega_L) + \frac{\mathrm{Im} f}{|1 - f(\beta^2 g_L - G_L)|^2} \right] + 2N(0)\langle \,|\, \delta\gamma^A \,|^2\rangle \mathrm{Im} f \, , \tag{41a}$$

where S_L is the strength of the exciton pole and obeys

$$S_L^{-1}=2\beta_L g_L+(\beta_L^2 g_L-G_L)\left[\frac{d\ln f}{d\beta}\right]_{\beta=\beta_L}. \tag{41b}$$

The integrated contribution of the first term in large parentheses in (41a) is $2\Delta\pi S_L$. It should be compared with

$$\int_{2\Delta}^{\infty}\mathrm{Im}f\,d\omega=2\Delta\pi(\pi/4)\,, \tag{42}$$

which is the integrated contribution of the second term when g_L and G_L tend to zero. When g_L and G_L are nonzero, the presence of f in the denominator of the second term of (41a) removes the singular peak from the numerator at $\omega=2\Delta$ and reduces the integrated contribution below that given by (42).

We now discuss the possibility that the E_g Raman gap peak observed by Dierker *et al.*[15] is due to an E_g-symmetry exciton rather than to gap anisotropy. Since the E_g peak is about 20% lower in energy than the A_{1g} and T_{2g} peaks, we set $\beta_L=0.8$. We assume $G_0=0.4$ and find that Eq. (40) has two solutions for G_L, namely

$$G_L=0.305,-0.679\,. \tag{43a}$$

Equation (48b) then gives

$$S_L=0.256,0.690\,, \tag{43b}$$

respectively. Thus the repulsive interaction gives a strength to the exciton peak almost as strong as that $(\pi/4)$ for the $G_L=0$ case.

Figure 14 compares the prediction of Eq. (41a) for a single nonzero $G_L=-0.679$ with that for $G_L=0$. In the latter, case, the E_g-weighted gap distribution, in the sense of Eq. (38c), was assumed to be a Gaussian with a $\approx 20\%$ lower mean and a width used to fit the E_g Raman spectrum of Nb_3Sn by Dierker *et al.* In both cases the theoretical expression was convoluted with a Gaussian to mimic the spectrometer response function. The double-peaked—exciton case is seen to be a bad approximation to the curve that fits the data well. We can exclude the possibility that the E_g spectrum in Nb_3Sn is due to an exciton with an isotropic gap.

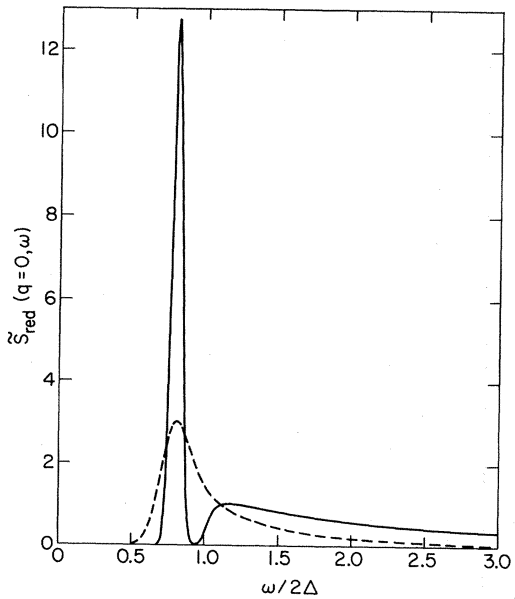

FIG. 14. $\tilde{S}_{\mathrm{red}}(q=0,\omega)$ vs $\omega/2\Delta$ for a single exciton at $\omega_L/2\Delta=0.8$ (solid line) compared with the prediction of Eqs. (41f) and (41g) (dashed line) which fits the E_g Raman spectrum of Nb_3Sn by Dierker *et al.* (Refs. 13 and 15) well.

In the case of an exciton with an anisotropic gap, Eq. (38a) must be used, and modeling is difficult. The singularity of f at $\omega=2\Delta$ is smeared out considerably for ω within the range of $2\Delta_k$. For a given value of G_L, gap anisotropy will shift the exciton resonance frequency ω_L upward and weaken S_L. The resonance will acquire a finite width if ω_L lies within the range of $2\Delta_k$, and for small $|G_L|$, the resulting spectrum will not differ much from that of a model with an anisotropic gap and no excitons. A small excitonic effect cannot be excluded, but we conclude that the main reason for the downward shift in the E_g peak is gap anisotropy.

IV. PHONON SELF-ENERGY

As discussed in the Introduction, the experiments of Sooryakumar and Klein[8–10] suggest that in $2H$-$NbSe_2$ the superconducting gap excitations acquire their Raman activity by coupling to Raman-active amplitude modes of the CDW. The Raman activity of the latter can, in turn, be related to the strong two-phonon scattering in the normal phase of those phonons that ultimately condense to form the CDW.[30] We therefore assume that the direct Raman activity of the gap excitations in $2H$-$NbSe_2$ as described in Secs. II and III is weaker than that acquired via the CDW phonons. We need to calculate the phonon Green's function in the presence of coupling to the superconducting electrons. If the CDW phonon behaves as ordinary $q\sim 0$ optical phonons, the interaction will take the form

$$H'=\tilde{\rho}_q b_q+\mathrm{H.c.}\,, \tag{44a}$$

where now

$$\tilde{\rho}_q=\sum_{k,\sigma} c^{\dagger}_{k+q,\sigma}c_{k\sigma}g_k\,. \tag{44b}$$

In Eq. (44b), g_k is the matrix element for an electron which scatters from k to $k+q$, and b_q is the phonon's destruction operator. In the Nambu representation Eqs. (44a) and (44b) are equivalent to a bare electron-phonon vertex of the form

$$\underline{g}(k)=g_k\underline{\tau}_3\,. \tag{44c}$$

The full vertex function Λ corresponding to (44c) will obey an equation such as (12) with $\underline{\gamma}(k)$ replaced by $\underline{g}(k)$. We shall denote this by $\Lambda(g)$. The resulting polarization,

$$\Pi(q,\omega)=B_{\Lambda(g),g^*}(q,\omega)\,, \tag{45}$$

is the phonon self-energy as corrected for the residual electron-electron interaction and as screened by the Coulomb interaction.

We go to the $q=0$ limit and obtain from Eq. (34e)

$$\Pi(0,\omega)=-2N(0)[\langle f\,|\,\delta g^{A}\,|^{2}\rangle-\langle f\delta g^{A}\rangle\langle f\delta g^{A*}\rangle/\langle f\rangle]$$
$$-2N(0)\sum_{\Gamma\neq A}\langle f\,|\,\delta g^{\Gamma}\,|^{2}\rangle\ , \tag{46a}$$

where $\delta g_k\equiv g_k-\langle g\rangle$ and where δg^{Γ} is that part of δg belonging to irreducible representation Γ. For an isotropic gap Eq. (46a) further simplifies to

$$\Pi(0,\omega)=-2N(0)\langle\,|\,\delta g\,|^{2}\rangle f\ , \tag{46b}$$

where f is given by Eqs. (9a) and (9b) as

$$f=\beta^{-1}(1-\beta^{2})^{-1/2}\sin^{-1}\beta\ ,\quad \beta=\omega/(2\Delta)\ .$$

In their theory of the coupling of the 2Δ gap excitations to CDW phonons, Balseiro and Falicov used the coupling in Eqs. (44a) and (44b) with $q=0$ and $g_k=g$, a constant.[11] They used the bare vertex and obtained the result

$$\Pi(0,\omega)=-2N(0)g^{2}f\ . \tag{46c}$$

When used to calculate the phonon Green's function $D(q,\omega)$ via

$$[D(q,\omega)]^{-1}=\frac{\omega^{2}-\omega_0(q)^{2}}{2\omega_0(q)}-\Pi(q,\omega)\ , \tag{47a}$$

Eq. (46c) gives a pole in $D(0,\omega)$ at a frequency $\omega_p<2\Delta$, obeying

$$\omega_p^{2}=\omega_0^{2}-4\omega_0N(0)g^{2}4\Delta^{2}\frac{\sin^{-1}(\omega_p/2\Delta)}{\omega_p(4\Delta^{2}-\omega_p^{2})^{1/2}}\ . \tag{47b}$$

Here ω_0 is the unrenormalized phonon frequency at $q=0$.

As pointed out by Littlewood and Varma,[12] this model cannot be used as is, because vertex (and Coulomb) corrections will completely screen the constant electron-phonon interaction g. We see, however, from Eq. (46b), that if g_k is anisotropic on the Fermi surface, then the Balseiro-Falicov calculation of $\Pi(0,\omega)$ and others based on it[9] may be generalized if their parameter g^{2} is reinterpreted to be $\langle\,|\,\delta g\,|^{2}\rangle$. The rough fits to the experimental data require[11,9]

$$N(0)\langle\,|\,\delta g\,|^{2}\rangle\approx 0.1\hbar\omega_0\ . \tag{48}$$

One expects an anisotropic g_k in the CDW state, with the largest $|\,g_k\,|$'s on those parts of the Fermi surface affected most by the formation of the CDW.

Littlewood and Varma pointed out that another type of coupling should be expected between quasiparticle pairs and CDW amplitude modes.[12] They argued that on those parts of the Fermi surface most affected by the CDW, the amplitude mode of the CDW will modulate the local value of the electronic density of states and hence the gap via equations such as our (20c) and (20b). The resulting vertex is proportional to Nambu's $\underline{\tau}_1$. Such a coupling gives rise to another collective mode with frequency $2\Delta/\hbar$ at $q=0$, which becomes damped at finite q,[12] and whose dispersion was calculated (for superfluid He^3) by Brusov and Popov.[31]

Recently, Browne and Levin have treated the CDW and superconductivity self-consistently within a random-phase approximation.[32] Treating the CDW within a one-dimensional approximation, they succeeded in deriving microscopically a coupling of the type considered by Littlewood and Varma.[12] A similar but independent calculation has been done by Kurihara.[33]

It is also of interest to correct the vertex $\underline{\Gamma}(k_+,k_-)$ for both phonon and Coulomb polarizations. Let $\underline{\Omega}(k_+,k_-)$ denote this corrected vertex. It will obey an equation such as (12) with the following additional term on the right-hand side:

$$\underline{g}(\vec{k})\underline{\tau}_3B_{\Omega g^*}D_0(q,\omega)\ , \tag{49}$$

where $D_0(q,\omega)$ is the bare phonon Green's function. The formal solution for Ω is

$$\underline{\Omega}=\underline{\Gamma}+V_qB_{\Omega 1}\underline{\Gamma}(1)+D_0(q,\omega)B_{\Omega g^*}\underline{\Gamma}(g(k))\ , \tag{50}$$

where $\underline{\Gamma}(g(k))$ is the corrected vertex for $\underline{\tau}_3g(\vec{k})$. From Eq. (50) one can form the polarizations $B_{\Omega 1}$ and $B_{\Omega g^*}$ and solve the resulting two equations for them. One can then form the polarization $B_{\Omega\gamma^*}$ from Eq. (50) and obtain after some rearrangement

$$B_{\Omega\gamma^*}=B_{\Lambda\gamma^*}+B_{\Lambda g^*}D(q,\omega)B_{\Lambda(g)\gamma^*}\ . \tag{51}$$

Here $B_{\Lambda\gamma^*}$ is the Coulomb-corrected polarization given by Eq. (17), $B_{\Lambda g^*}$ is given by Eq. (17) with γ^* replaced by g^*, and $B_{\Lambda(g)\gamma^*}$ is given by Eq. (17) with Γ replaced by $\Gamma(g)$. $D(q,\omega)$ obeys Eqs. (47a) and (45).

When the "imaginary part" of $B_{\Omega\gamma^*}$ is calculated, following the prescription of Eq. (6d), the second term in Eq. (51) gives both phonon Raman scattering [from $\mathrm{Re}(B_{\Lambda g^*}B_{\Lambda(g)\gamma^*})\mathrm{Im}D(q,\omega)$] and electronic Raman scattering [from $\mathrm{Re}D(q,\omega)\mathrm{Im}(B_{\Lambda g^*}B_{\Lambda(g)\gamma^*})$]. The latter contribution will, in general, interfere with $\mathrm{Im}B_{\Lambda\gamma^*}$ from the first term in Eq. (51). Because of the complicated band structure of transition metals and transition-metal compounds, the phonon contribution must include the interband generalizations of $B_{\Lambda g^*}$ and $B_{\Lambda(g)\gamma^*}$.[34]

V. CONCLUSIONS

We have derived general expressions such as Eq. (28d) which, in principle, allow a calculation of the Raman spectral function [by use of Eq. (6d)] for finite wave-vector transfer $\vec{q}$ and with inclusion of coupling constant and gap anisotropy and vertex and Coulomb-polarization corrections. Useful expressions and numerical results were obtained only by giving up full generality, namely for finite q and no anisotropy (Appendix B and Ref. 18) or for anisotropy, but with $q\sim 0$ [Eqs. (34f) and (34g)]. Fortunately, the study of the q dependence in Appendix B and in Ref. 18 gives us confidence that the $q\sim 0$ limit applies almost literally for wave-vector transfers equal to ξ^{-1} or less and optical penetration depths equal to ξ or larger. Thus it applies well for $2H$-$NbSe_2$, Nb_3Sn, V_3Si, and to other clean superconductors that have short coherence lengths ξ. Such a superconductor should have an almost singular peak in the Raman spectrum at $\omega=2\Delta$. For good practical results, the Raman matrix element must also be anisotropic so that $\langle\,|\,\delta\gamma_k\,|^{2}\rangle$ will be large. Since the Raman intensity is proportional to $N(0)$, those super-

conductors with a large density of states will be favored in a Raman experiment.

Similar conditions [$q\xi < 1$, large $N(0)$], in addition to a large value of the coupling constant $\langle |\delta g_k|^2 \rangle$, favor a strong peak below 2Δ in the spectral function of an optical phonon.

ACKNOWLEDGMENTS

We have enjoyed stimulating discussions with C. M. Varma, P. B. Littlewood, A. J. Leggett, D. A. Browne, and K. Levin. This work was supported by the National Science Foundation under Grant No. DMR-80-20250. One of us (S.B.D.) would like to acknowledge the support of University fellowships and a General Electric Foundation fellowship.

APPENDIX A: FURTHER EVALUATION OF EXPRESSION FOR $\tilde{S}(\vec{q},\omega)$

The integrand in Eq. (2a) makes a contribution only for k near the Fermi surface. Its only rapid k dependence is through its dependence on the energy ϵ_k, as long as the group velocity v_k is not so small as to give a rapidly varying density of states $N(\epsilon)$ near $\epsilon=0$. Excluding this possibility, we may write, for $F(\epsilon_k,\vec{k})$, the integrand in Eq. (2a),

$$\int d^3k\, F(\epsilon_k,\vec{k}) = \int d^3k \int \delta(\epsilon_k-\epsilon)F(\epsilon,\vec{k})d\epsilon \approx \int d^3k\, \delta(\epsilon_k)\int_{-\infty}^{\infty} F(\epsilon,\vec{k})d\epsilon \,. \quad \text{(A1)}$$

In addition, we may consider E of Eq. (2b) to be the integration variable by using the identity

$$\int_{-\infty}^{\infty} F\,d\epsilon = \sum_{s=\pm1}\int_0^{\infty} \frac{FsE\,dE}{(E^2-\Delta_k^2)^{1/2}} \,, \quad \text{(A2a)}$$

where $s=\mathrm{sgn}(\epsilon)$. By defining

$$\Omega(E)=E+E'(E) \,, \quad \text{(A3a)}$$

where

$$E'(E)=[E^2+2\epsilon(\vec{q}\cdot\vec{v}_k)+(\vec{q}\cdot\vec{v}_k)^2]^{1/2} \quad \text{(A3b)}$$

with

$$\epsilon = s(E^2-\Delta_k^2)^{1/2} \,, \quad \text{(A3c)}$$

we have

$$\delta(\omega-E-E')=\delta(\omega-\Omega(E))=\delta(E-E_0)\left|\frac{dE}{d\Omega}\right|_{\Omega=\omega} \,, \quad \text{(A4a)}$$

where E_0 is the value of E that satisfies

$$\omega = E_0+E'(E_0) \,. \quad \text{(A4b)}$$

We find that

$$2(\vec{q}\cdot\vec{v}_k)s(E^2-\Delta_k^2)^{1/2}=\Omega^2-2\Omega E-(\vec{q}\cdot\vec{v}_k)^2 \,. \quad \text{(A5)}$$

We differentiate both sides of Eq. (A5) with respect to Ω and obtain

$$\left|\frac{dE}{d\Omega}\right|_{\Omega=\omega} = \frac{(\omega-E_0)(E_0^2-\Delta_k^2)^{1/2}}{|sE_0(\vec{q}\cdot\vec{v}_k)+(E_0^2-\Delta_k^2)^{1/2}|} \,. \quad \text{(A6)}$$

Using Eqs. (A2), (A3), (A4), and (A6) in Eq. (2a), we obtain

$$\tilde{S}(\vec{q},\omega)=\tfrac{1}{2}\sum_{s=\pm1}\int \frac{d^3k}{(2\pi)^3}\delta(\epsilon_k)|\gamma_k|^2 \times \frac{[E_0(\omega-E_0)+\Delta_k^2-\epsilon\epsilon']s}{|sE_0(\vec{q}\cdot\vec{v}_k)+\omega(E_0^2-\Delta_k^2)^{1/2}|} \,. \quad \text{(A7)}$$

By the use of Eq. (A5) we obtain, for the expression in the denominator of Eq. (A7),

$$|sE_0(\vec{q}\cdot\vec{v}_k)+\omega(E_0^2-\Delta_k^2)^{1/2}| = sW\frac{\omega^2-(\vec{q}\cdot\vec{v}_k)^2}{2|\vec{q}\cdot\vec{v}_k|} \,, \quad \text{(A8a)}$$

where

$$W\equiv\omega-2E_0 \,. \quad \text{(A8b)}$$

From Eq. (A5) with $E=E_0$ and $\Omega=\omega$, we find that W obeys

$$2(\vec{q}\cdot\vec{v}_k)s\left[\frac{\omega^2}{4}-\frac{W\omega}{2}+\frac{W^2}{4}-\Delta_k^2\right]^{1/2}=\omega W-(\vec{q}\cdot\vec{v}_k)^2 \,. \quad \text{(A9a)}$$

This may be solved for W, giving

$$W=|\vec{q}\cdot\vec{v}_k|[\omega^2-(\vec{q}\cdot\vec{v}_k)^2-4\Delta_k^2]^{1/2} \times[\omega^2-(\vec{q}\cdot\vec{v}_k)^2]^{-1/2} \,. \quad \text{(A9b)}$$

Using $\epsilon'=\epsilon+(\vec{q}\cdot\vec{v}_k)$, we find, from Eq. (A3c),

$$\epsilon\epsilon'=s(E^2-\Delta_k^2)^{1/2}[s(E^2-\Delta_k^2)^{1/2}+(\vec{q}\cdot\vec{v}_k)] \,. \quad \text{(A10a)}$$

We eliminate $s(E^2-\Delta_k^2)^{1/2}$ by use of Eq. (A5) and obtain, from (A10a),

$$\epsilon\epsilon'=[(\omega W)^2-(\vec{q}\cdot\vec{v}_k)^4]/4(\vec{q}\cdot\vec{v}_k)^2 \,. \quad \text{(A10b)}$$

Use of (A8b) gives

$$E_0=(W-\omega)/2$$

and

$$\omega-E_0=(\omega+W)/2 \,.$$

Thus

$$E_0(\omega-E_0)=(\omega^2-W^2)/4 \,. \quad \text{(A10c)}$$

Equations (A10b) and (A10c) together with (A9) then give

$$E_0(\omega-E_0)+\Delta_k^2-\epsilon\epsilon'=2\omega^2\Delta_k^2[\omega^2-(\vec{q}\cdot\vec{v}_k)^2]^{-1} \,. \quad \text{(A10d)}$$

Use of Eqs. (A10d), (A8a), (A9a), and (A9b) in (A7) then gives

$$\tilde{S}(\vec{q},\omega)=4\omega^2\int' \frac{d^3k}{(2\pi)^3}\frac{\delta(\epsilon_k)|\gamma_k|^2\Delta_k^2}{[\omega^2-(\vec{q}\cdot\vec{v}_k)^2]^{3/2}[\omega^2-(\vec{q}\cdot\vec{v}_k)^2-4\Delta^2]^{1/2}} \,. \quad \text{(A10e)}$$

APPENDIX B: EVALUATION OF $\tilde{S}(q,\omega)$ FOR THE ISOTROPIC BCS CASE.

Introducing the angle θ between $\vec{q}$ and $\vec{v}_k$, and defining the variable z by

$$z=\frac{qv\cos\theta}{(\omega^2-4\Delta^2)^{1/2}}\ , \tag{B1a}$$

we find from Eq. (3) for $\Delta_k=\Delta$, $\gamma_k=\gamma$, and $|\vec{v}_k|=v$, and for a spherical Fermi surface,

$$\tilde{S}(q,\omega)=2N(0)\gamma^2\frac{2\Delta^2}{qv\omega}\int_0^{z_0}\frac{dz}{(1-mz^2)^{3/2}(1-z^2)^{1/2}}\ , \tag{B1b}$$

where

$$z_0=\min\left[1,\frac{qv}{(\omega^2-4\Delta^2)^{1/2}}\right]\ ,\quad m=1-4\Delta^2/\omega^2\ . \tag{B1c}$$

When $(4\Delta^2+(qv)^2)^{1/2}>\omega>2\Delta$, we have $z_0=1$, and the integral is expressible in terms of complete elliptic integrals,

$$\begin{aligned}\tilde{S}(q,\omega)&=N(0)\gamma^2\frac{\omega}{qv}E(1-4\Delta^2/\omega^2)\\&=\frac{2N(0)\gamma^2}{qv}\left[\left[\frac{\omega}{2}+\Delta\right]E\left[\frac{\omega-2\Delta}{\omega+2\Delta}\right]-\frac{2\Delta\omega}{\omega+2\Delta}K\left[\frac{\omega-2\Delta}{\omega+2\Delta}\right]\right]\ .\end{aligned} \tag{B2}$$

At $\omega=2\Delta$, $\tilde{S}(q,\omega)$ jumps discontinuously from zero to $\gamma^2 2N(0)\Delta(qv)^{-1}(\pi/2)$, which is $\pi/2$ larger than the normal-metal value $N(0)\gamma^2\omega(qv)^{-1}$. $\tilde{S}(q,\omega)$ rises as ω increases. When $\omega=(4\Delta^2+(qv)^2)^{1/2}$, there is a sharp discontinuity in slope.

When $\omega>(4\Delta^2(qv)^2)^{1/2}$, we have $z_0=qv/(\omega^2-4\Delta^2)^{1/2}$, and introducing the incomplete elliptic integral,

$$E(\phi\backslash\alpha)=\int_0^{\phi}(1-\sin^2\alpha\sin^2\theta)^{1/2}d\theta\ , \tag{B3a}$$

where

$$\phi=\sin^{-1}z_0\ \text{ and }\ \sin^2\alpha=m, \tag{B3b}$$

we find

$$\tilde{S}(q,\omega)=N(0)\gamma^2\left[\frac{\omega}{qv}E(\phi\backslash\alpha)-\frac{(\omega^2-4\Delta^2-q^2v^2)^{1/2}}{(\omega^2-q^2v^2)^{1/2}}\right]\ . \tag{B4}$$

This is a decreasing function of ω, unlike Eq. (B2), which gives an increasing function.

When $q\to 0$, we obtain, from (B4),

$$\tilde{S}(q\to 0,\omega)=\frac{2N(0)\gamma^2 2\Delta^2}{(\omega^2-4\Delta^2)^{1/2}\omega}\ , \tag{B5}$$

which may also be obtained directly from Eq. (3c). The behavior of $\tilde{S}(q,\omega)$ is shown in Fig. 1 for $q\xi=0.1$, 0.5, 1.0, 2, 4, and 8 where $\xi=v(2\Delta)^{-1}$ is the coherence length.

*Present address: AT&T Bell Laboratories, Murray Hill, New Jersey 07974.

[1]J. Bardeen, L. N. Cooper, and J. R. Schrieffer, Phys. Rev. 108, 1175 (1957).

[2]A. A. Abrikosov and L. A. Fal'kovskii, Zh. Eksp. Teor. Fiz. 40, 262 (1961) [Sov. Phys.—JETP 13, 179 (1961)].

[3]S. Y. Tong and A. A. Maradudin, Mater. Res. Bull. 4, 563 (1969).

[4]D. R. Tilley, Z. Phys. 254, 71 (1972); J. Phys. F 38, 417 (1973).

[5]A. A. Abrikosov and V. M. Genkin, Zh. Eksp. Teor. Fiz. 65, 842 (1973) [Sov. Phys.—JETP 38, 417 (1974)].

[6]C. B. Cuden, Phys. Rev. B 13, 1993 (1976); *ibid.* 18, 3156 (1978).

[7]L. M. Fraas, P. F. Williams, and S. P. S. Porto, Solid State Commun. 8, 2113 (1970).

[8]R. Sooryakumar and M. V. Klein, Phys. Rev. Lett. 45, 660 (1980).

[9]R. Sooryakumar and M. V. Klein, Phys. Rev. B 23, 3213 (1981).

[10]R. Sooryakumar, M. V. Klein, and R. F. Frindt, Phys. Rev. B 23, 3222, (1981).

[11]C. A. Balseiro and L. M. Falicov, Phys. Rev. Lett. 45, 662 (1980).

[12]P. B. Littlewood and C. M. Varma, Phys. Rev. Lett. 47, 811 (1981); Phys. Rev. B 26, 4883 (1982).

[13]M. V. Klein, in *Superconductivity in d- and f-Band Metals,* edited by W. Buckel and W. Weber (Kernforschungszentrum Karlsruhe, Karlsruhe, Federal Republic of Germany, 1982), p. 539.

[14]S. B. Dierker, M. V. Klein, G. Webb, Z. Fisk, J. Wernick, G. Hull, J.-E. Jørgensen, and S. R. Rasmussen, in *Superconductivity in d- and f-Band Metals,* Ref. 13, p. 563.

[15]S. B. Dierker, M. V. Klein, G. W. Webb, and Z. Fisk, Phys. Rev. Lett. 50, 853 (1983).

[16]R. Hackl, R. Kaiser, and S. Schicktanz, in *Superconductivity in d- and f-Band Metals,* Ref. 13, p. 559.

[17]R. Hackl, R. Kaiser, and S. Schicktanz, J. Phys. C 16, 1729 (1983).

[18]S. B. Dierker, Ph.D. thesis, University of Illinois, 1983.

[19]D. L. Mills, A. A. Maradudin, and E. Burstein, Ann. Phys. (N.Y.) 56, 504 (1970).

[20]A. A. Abrikosov, L. P. Gorkov, and I. E. Dzyaloshinski, *Methods of Quantum Field Theory in Statistical Physics* (Dover, New York, 1963).

[21]Y. Nambu, Phys. Rev. 117, 648 (1960).

[22]A. Kawabata, J. Phys. Soc. Jpn. 30, 68 (1971).

[23]M. V. Klein, Phys. Rev. B 24, 4208 (1981).

[24]V. G. Vaks, V. M. Galitskii, and A. I. Larkin, Zh. Eksp. Teor. Fiz. 41, 1655 (1961) [Sov. Phys.—JETP 14, 1177 (1962)].

[25]P. B. Allen, Phys. Rev. B 13, 1416 (1976).

[26]N. N. Bogoliubov, Nuovo Cimento 7, 6 (1958); 7, 794 (1958); N. N. Bogoliubov, V. V. Tolmachev and D. V. Shirkov, *A New Method in the Theory of Superconductivity* (Consultants Bureau, New York, 1959).

[27]P. W. Anderson, Phys. Rev. 112, 1900 (1958).

[28]A. Bardasis and J. R. Schrieffer, Phys. Rev. 121, 1050 (1961).

[29]For a general discussion see P. C. Martin in *Superconductivity,* edited by R. D. Parks (Dekker, New York, 1969), Vol. 1, p.

371.
[30]M. V. Klein, Phys. Rev. B 25, 7192 (1982).
[31]P. N. Brusov and V. N. Popov, Zh. Eksp. Teor. Fiz. 78, 2419 (1980) [Sov. Phys.—JETP 51, 1217 (1980)].
[32]D. A. Browne and K. Levin, Phys. Rev. B 28, 4029 (1983).
[33]Y. Kurihara, J. Phys. Soc. Jpn. 52, 542 (1983).
[34]M. V. Klein, in *Light Scattering in Solids III*, edited by M. Cardona and G. Güntherodt (Springer, Berlin, 1982) p. 136.